JOURNAL OF SOLID STATE CHEMISTRY 88, 384–390 (1990)

High Pressure Synthesis and Electrical and Magnetic Properties of $MnGe_4$ and $CoGe_4$

H. TAKIZAWA, T. SATO, T. ENDO, AND M. SHIMADA

Department of Molecular Chemistry and Engineering, Faculty of Engineering, Tohoku University, Aoba-ku, Sendai, Miyagi 980, Japan

Received January 2, 1990; in revised form May 25, 1990

The new germanides, $MnGe_4$ and $CoGe_4$, were synthesized by solid state reactions at 5.5–6 GPa and 600–700°C for 2 hr using the belt-type high pressure apparatus. The crystal structures of $MnGe_4$ and $CoGe_4$ are superstructures of the β-$NiHg_4$-type structures. The unit cell of $MnGe_4$ is composed of four β-$NiHg_4$-type cells and that of $CoGe_4$ is composed of eight β-$NiHg_4$-type cells. $MnGe_4$ is a metallic conductor and an itinerant electron ferromagnet with a Curie temperature of 340 K. $CoGe_4$ is a metallic conductor and a Pauli paramagnet.

Introduction

There have been a number of investigations about the preparations and the physical properties of intermetallic compounds in the binary transition metal–4B metalloid atom systems. Transition metal silicides, especially, have been widely investigated because of their various kinds of electrical and magnetic properties and their potential application in solid state electronic devices (*1, 2*).

Although crystal structure and physical properties of transition metal germanides are expected to be similar to those of transition metal silicides, no systematic investigations have yet been carried out. Transition metal germanides have various chemical compositions represented by formulas such as T_3Ge, T_2Ge, T_5Ge_3, $T_{11}Ge_8$, TGe, TGe_2, and TGe_4 (T: transition metal). Among these germanides, the compounds containing more than 67 at.% Ge were rarely investigated. Only two compounds, $IrGe_4$ and $RhGe_4$, were synthesized (*3, 4*). Recent investigations on synthesis of transition metal germanides demonstrate that the high pressure synthesis is a suitable method for the preparation of new germanides with high germanium contents (*5–7*).

In the present study, $MnGe_4$ and $CoGe_4$ were synthesized under high pressure–temperature conditions, and their electrical and magnetic properties were investigated.

Experimental

Manganese and cobalt powders (>99.9% purity) and germanium powder (>99.99% purity) were mixed with Ge/T (T: Mn, Co) atomic ratios varying from 4.0 to 5.0 using an agate mortar and uniaxially pressed at 100 MPa at room temperature to form pellets, 5 mm in diameter and 3 mm in thickness. The pellets were put into a cylindrical BN capsule, which was placed in a carbon heater. The assemblage was put into a cell constructed with NaCl and subjected to high

0022-4596/90 $3.00

pressure–temperature conditions using the belt-type high pressure apparatus. The high pressure–temperature treatments were carried out at 5.5–6 GPa and 600–700°C for 2 hr, and then the samples were quenched to room temperature prior to releasing the applied pressure. The detailed preparation procedures were described in the previous paper (*5*).

The pellets thus obtained were pulverized and the residual germanium was removed by leaching with 5 *N* NaOH + 3% H_2O_2 solutions at room temperature. Chemical analysis was carried out by means of ICP emission spectrochemical analysis.

The phase of product was identified by X-ray powder diffraction analysis using Ni-filtered Cu$K\alpha$ radiation or Fe-filtered Co$K\alpha$ radiation. Lattice parameters were determined by a least-squares method using silicon as an internal standard.

The electrical resistivity was measured by a standard four-probes method in the temperature range 77–400 K. Magnetization and magnetic susceptibility were measured by a magnetic torsion balance in magnetic field up to 10 kOe in the temperature range 77–450 K.

TABLE I

X-RAY POWDER DIFFRACTION DATA OF $MnGe_4$

d_{obsd} (nm)	d_{calcd} (nm)	h	k	l	I_{obsd}
0.551	0.5515	2	0	0	vvw
0.500	0.4992	1	0	1	vw
0.3072	0.3073	3	0	1	m
0.2800	0.2799	0	0	2	s
0.2757	0.2757	4	0	0	vs
0.2496	0.2496	2	0	2	w
0.2469	0.2466	4	2	0	w
0.2416	0.2414	4	1	1	w
0.2051	0.2052	4	3	1, 5 0 1	vw
0.1965	0.1964	4	0	2	vvs
0.1951	0.1950	4	4	0	s
0.1839	0.1839	1	0	3, 6 0 0	w
0.1600	0.1600	4	4	2	m
0.1425	0.1425	4	3	3, 5 0 3	w
0.1400	0.1400	0	0	4	w
0.1378	0.1378	5	2	3, 8 0 0	w
0.1342	0.1342	6	4	2	w
0.1329	0.1329	7	4	1, 8 1 1	vw
0.1265	0.1266	5	4	3	vw
0.1248	0.1248	4	0	4	w
0.1237	0.1237	8	0	2	w
0.1234	0.1233	6	3	3, 8 4 0	w
0.1204	0.1204	7	0	3	vw
0.1138	0.1137	4	4	4	w
0.1129	0.1128	8	4	2	m
0.1113	0.1114	1	0	5, 6 0 4	vw
0.1104	0.1103	7	4	3, 8 1 3,10 0 0	w
0.1072	0.1071	3	0	5	vw
0.1033	0.1033	4	1	5, 6 4 4	vw
0.1026	0.1026	8	6	2,10 0 2	vw
0.1024	0.1024	9	0	3,10 4 0	vw

Experimental Results

$MnGe_4$

$MnGe_4$ was synthesized at 5.5 GPa and 600–700°C for 2 hr. The product obtained from the reaction with the starting composition of Ge/Mn = 4.0 contained small amounts of Mn_3Ge_5 and $MnGe_2$. A single phase of $MnGe_4$ was obtained from the product with the starting composition of Ge/Mn = 4.8 by leaching out the residual germanium. The germanium content of the single phase sample was analyzed to be 85.8 ± 0.1 wt% Ge, which was relatively higher than the calculated value of 84.1 wt% Ge in $MnGe_4$.

The X-ray powder diffraction data of $MnGe_4$ are listed in Table I. All diffraction peaks of $MnGe_4$ could be completely indexed in the tetragonal structure with lattice constants of $a = 1.103 \pm 0.001$ and $c = 0.5598 \pm 0.0003$ nm, respectively. Since the observed reflections satisfied the condition of $h + k + l = 2n$, the space group is expected to be one of $I4/m$, $I422$, $I4mm$, $I\bar{4}m2$, $I\bar{4}2m$, or $I4/mmm$.

$MnGe_4$ was metastable under ambient pressure condition and decomposed into Mn_5Ge_3 and Ge at 270–300°C.

The results of magnetization measurements of $MnGe_4$ are shown in Figs. 1 and

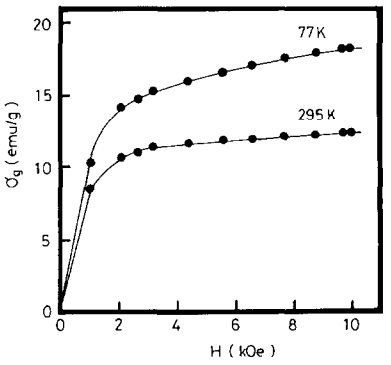

FIG. 1. Magnetic field dependence of magnetization of $MnGe_4$.

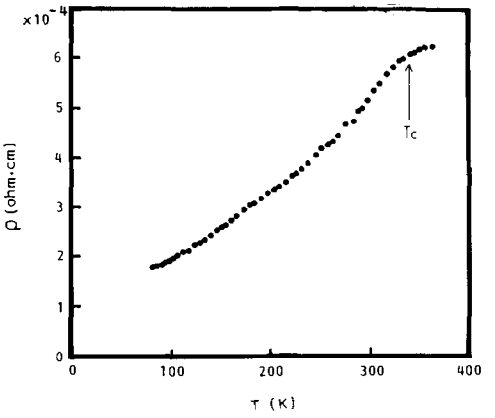

FIG. 3. Temperature dependence of electrical resistivity of $MnGe_4$.

2. $MnGe_4$ exhibited ferromagnetic behavior with a Curie temperature of 340 K. The saturation magnetic moment, μ_s, of Mn atom extrapolated to 0 K was calculated to be 1.2 $\pm$ 0.1 μ_B. Above the Curie temperature, the magnetic susceptibility followed the Curie–Weiss-type law $M\chi_g = M\chi_c + C/(T - \Theta_p)$, where M is the formula weight and χ_c is the temperature-independent magnetic susceptibility. The number of effective Bohr magnetons, P_{eff}, and the paramagnetic Curie temperature, Θ_p, were calculated to be 2.83 $\pm$ 0.03 μ_B and 349 $\pm$ 3 K, respectively.

Figure 3 shows the results of the electrical resistivity measurement; $MnGe_4$ exhibits metallic conduction. The ρ–T curve was not linear in the measured temperature range; an anomaly was observed at the Curie temperature.

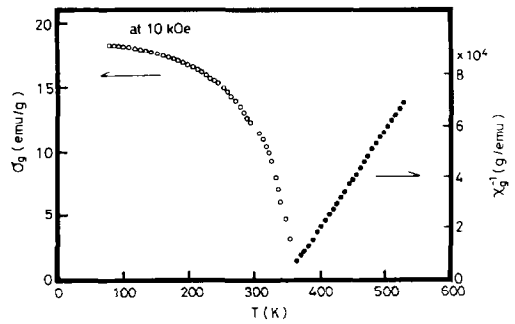

FIG. 2. Temperature dependence of magnetization and reciprocal magnetic susceptibility of $MnGe_4$.

$CoGe_4$

$CoGe_4$ was synthesized at 6 GPa and 600–700°C for 2 hr. Single phase $CoGe_4$ was obtained from the product with the starting composition of Ge/Co = 4.2 by leaching out the residual germanium. The germanium content of the single phase sample was analyzed to be 83.5 $\pm$ 0.1 wt% Ge, which was slightly higher than the calculated value of 83.1 wt% Ge in $CoGe_4$.

The X-ray powder diffraction data of $CoGe_4$ are listed in Table II. All diffraction peaks of $CoGe_4$ were completely indexed in the cubic structure with a lattice constant of a = 1.099 $\pm$ 0.001 nm. Since the observed reflections satisfied the condition $h + k + l = 2n$, the space group is expected to be one of $I23$, $I2_13$, $Im3$, $I432$, $I43m$, $Ia3$, or $Im3m$.

$CoGe_4$ was metastable under ambient pressure condition and decomposed into $CoGe_2$ and Ge at 380–400°C.

The temperature dependence of electrical resistivity of $CoGe_4$ is shown in Fig. 4. $CoGe_4$ shows metallic conduction with a linear temperature dependence of resistivity.

TABLE II

X-RAY POWDER DIFFRACTION DATA OF $CoGe_4$

d_{obsd} (nm)	d_{calcd} (nm)	h	k	l	I_{obsd}
0.449	0.4487	2	1	1	vw
0.318	0.3172	2	2	2	vw
0.2938	0.2937	3	2	1	m
0.2749	0.2748	4	0	0	vs
0.2592	0.2590	3	3	0, 4 1 1	vw
0.2459	0.2457	4	2	0	m
0.2157	0.2155	4	3	1, 5 1 0	vw
0.2007	0.2006	5	2	1	w
0.1944	0.1943	4	4	0	vvs
0.1832	0.1832	6	0	0, 4 4 2	w
0.1784	0.1783	6	1	1, 5 3 2	w
0.1587	0.1586	4	4	4	m
0.1497	0.1496	5	5	2, 6 3 3, 7 2 1	vw
0.1374	0.1374	8	0	0	m
0.1334	0.1333	6	4	4, 8 2 0	vw
0.1229	0.1229	8	4	0	m
0.1122	0.1122	8	4	4	m

The measurements of the magnetic susceptibility show that $CoGe_4$ is a Pauli paramagnetic with a magnetic susceptibility of 5×10^{-7} emu/g.

Discussion

Crystal Structures of $MnGe_4$ and $CoGe_4$

Some TX_4 compounds of the transition metal–4B metalloid atom systems have been synthesized. From the crystallographic point of view, these compounds are classified into three groups. $IrGe_4$ has the hexagonal structure with the space group of $P3_121$, which is closely related to defect-type γ-brass structure (*3*). $RhGe_4$ is isostructural with $IrGe_4$ (*4*). Stannides ($IrSn_4$, $PdSn_4$, and $PtSn_4$) have the orthorhombic $PtSn_4$-type structure (space group *Aba*2), which can be derived from the $CoGe_2$-type structure (*4*, *8–10*). $PtPb_4$ has the tetragonal structure with the space group of *P4/nbm*, which is derived from the $CuAl_2$-type structure (*11*). No further TX_4 compounds with other crystal structures than the above three types have been reported in the literature.

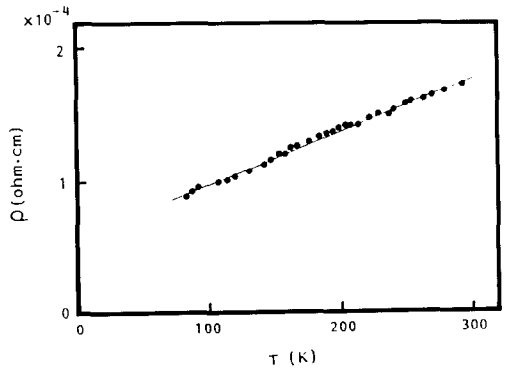

FIG. 4. Temperature dependence of electrical resistivity of $CoGe_4$.

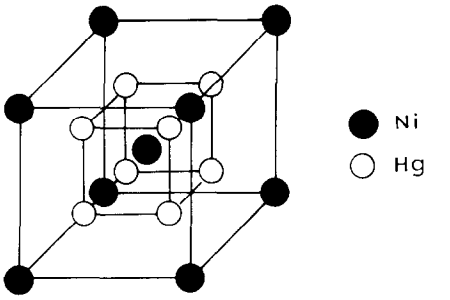

FIG. 5. Crystal structure of β-$NiHg_4$.

The crystal structures of $MnGe_4$ and $CoGe_4$ do not belong to the above-mentioned structure groups. The unit cells of $MnGe_4$ and $CoGe_4$ are considered to be superlattices of the β-$NiHg_4$-type cell. Figure 5 shows the crystal structure of β-$NiHg_4$. The β-$NiHg_4$ type is a filled up derivative of the *bcc* structure. Ni atoms form a *bcc* lattice and are surrounded by eight Hg atoms at the corners of a cube. The β-$NiHg_4$-type structure is found in $NiHg_4$, $PtHg_4$, $CrGa_4$, and $MnGa_4$ (*12*). Among these compounds, the atomic sizes of the constituent elements in $MnGa_4$ are almost the same as those in $MnGe_4$ and $CoGe_4$. The comparison of the sizes of the unit cells of $MnGa_4$, $MnGe_4$, and $CoGe_4$ is shown in Fig. 6. The size of the unit cells of $MnGe_4$ and $CoGe_4$ corre-

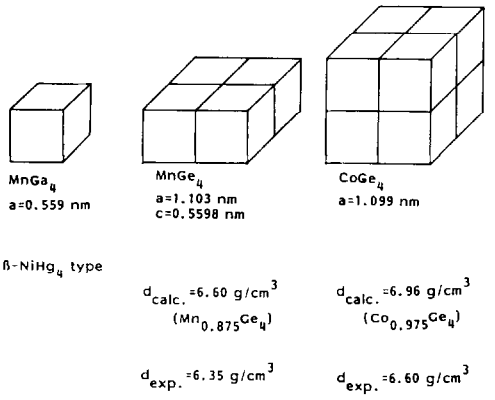

FIG. 6. Unit cells of $MnGe_4$ and $CoGe_4$ compared with the $MnGa_4$ structure (β-$NiHg_4$ type).

spond to four times and eight times that of $MnGa_4$, respectively.

Since the β-$NiHg_4$-type cell contains 2 formula units, the unit cells of $MnGe_4$ and $CoGe_4$ should contain 8 and 16 formula units, respectively. According to the present model, the theoretical densities of $MnGe_4$ and $CoGe_4$ were calculated to be 6.60 and 6.96 g/cm^3, respectively. The chemical formula units of the compounds were taken as $Mn_{0.875}Ge_4$ and $Co_{0.975}Ge_4$, which follows the results of chemical analysis. The pycnometrically measured densities of $MnGe_4$ and $CoGe_4$ were 6.35 and 6.60 g/cm^3, which agree with the calculated values within 5%.

Figure 7 shows the X-ray powder diffraction patterns of $MnGa_4$, $MnGe_4$, and $CoGe_4$. In the diffraction patterns of $MnGe_4$ and $CoGe_4$, the diffraction peaks corresponding to the strong diffraction peaks of $MnGa_4$ were also observed in $MnGa_4$ with the β-$NiHg_4$-type structure. This fact suggests that the crystal structures of $MnGe_4$ and $CoGe_4$ are the superstructures of the β-$NiHg_4$-type structure.

The absence of reflections (220) in the diffraction patterns of $MnGe_4$ and $CoGe_4$, which correspond to the (110) peak of $MnGa_4$, indicate that the slight positional changes of transition metal atoms from the ideal positions in the β-$NiHg_4$-type structure occur. It is plausible that the formation of the superstructures in $MnGe_4$ and $CoGe_4$ is due to vacancies at the transition metal sites and thus results in small positional changes of transition metal atoms. Since attempts of the single crystal growth of $MnGe_4$ and $CoGe_4$ under high pressure conditions were not successful, detailed structural analyses on single crystals were not possible.

Magnetic Properties of $MnGe_4$

$MnGe_4$ is a ferromagnetic with a Curie temperature of 340 K. The value of saturation magnetic moment, μ_s, does not agree with that of paramagnetic moment, μ_c, determined from the Curie–Weiss law. The curve of the magnetization against temperature is close to a Brillouin function and shows no evidence of ferrimagnetic behavior. The nonsaturating behavior of magnetization (see Fig. 1) can be explained by the itinerant electron theory of ferromagnetism (*13, 14*). In that case, the disagreement between μ_s and μ_c may be due to the spin fluctuation in the itinerant electron system.

In ferromagnets with the localized magnetic moment systems, μ_c/μ_s (Rhodes–Wohlfarth ratio) is 1. However, in an itinerant electron ferromagnet, μ_c/μ_s is larger than 1 (*15*). The relationship between μ_c/μ_s and T_c is characteristic of itinerant electron ferromagnets. The μ_c/μ_s values fall on a unique curve if plotted against the Curie temperature (*15*). Itinerant electron ferromagnets have wide distribution of properties, varying from "weakly ferromagnets," in which the T_c is low and the μ_c/μ_s is large, to "ferromagnets with nearly localized moment," in which the T_c is high and the μ_c/μ_s is nearly equal to 1 (*15, 16*). $MnGe_4$ ($\mu_c/\mu_s = 1.7$, $T_c = 340$ K) lies on the Rhodes–Wohlfarth curve and is situated in the intermediate region between weakly ferromagnets and nearly localized ferromagnets.

In itinerant electron systems, spin fluctu-

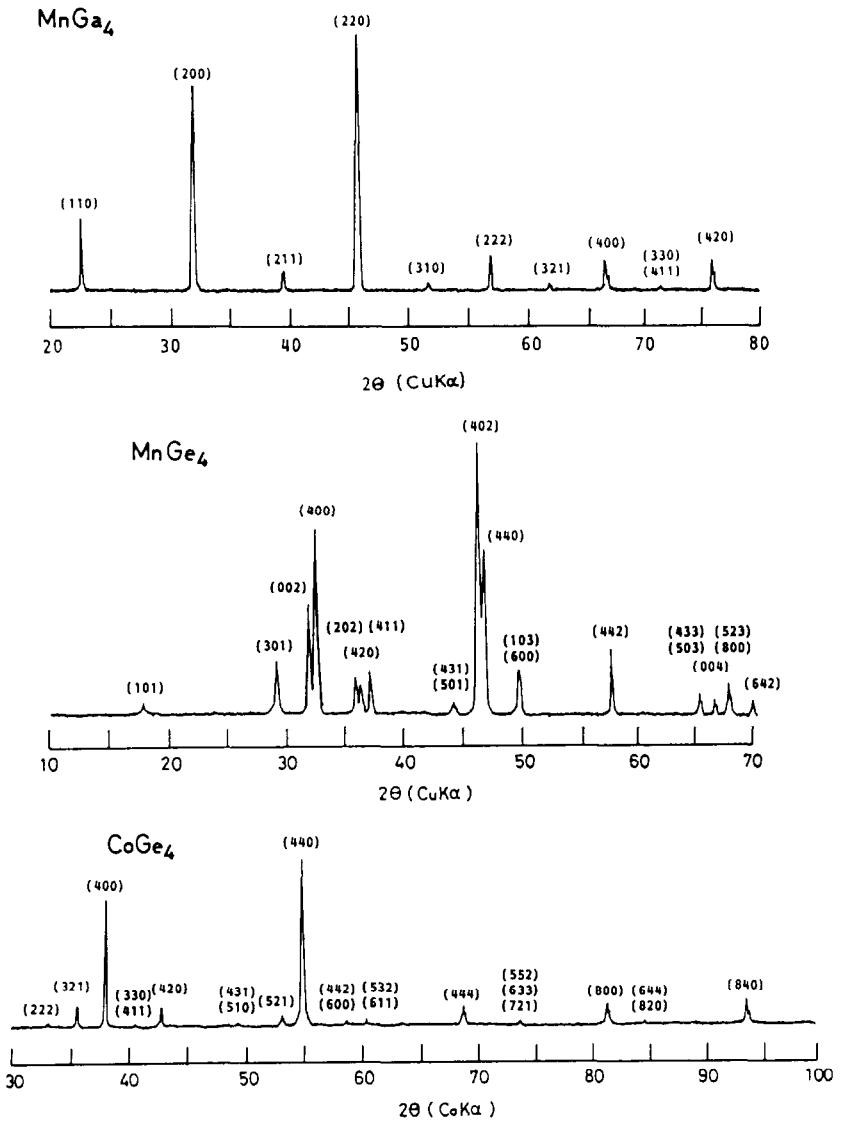

FIG. 7. X-ray powder diffraction patterns of $MnGa_4$, $MnGe_4$, and $CoGe_4$ ($CuK\alpha$ radiation for $MnGa_4$ and $MnGe_4$, $CoK\alpha$ for $CoGe_4$).

ations have an important effect upon the magnetic and transport properties of the compounds (*17–19*). A theory for the transport properties of weakly ferromagnets has been developed (*18*). However, no satisfactory theory has been proposed for itinerant electron ferromagnets belonging to the intermediate region between weak ferromagnets and nearly localized ferromagnets. The electrical resistivity, ρ, of a weak ferromagnet displays the relation ρ vs T^2 at low temperature and ρ vs $T^{5/3}$ at near T_c due to spin fluctuations (*18*). Although $MnGe_4$ is not really a weakly ferromagnet, a $T^{5/3}$ depen-

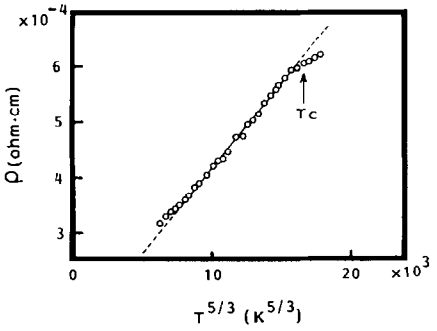

FIG. 8. ρ versus $T^{5/3}$ plots of $MnGe_4$.

dence of the electrical resistivity was observed in the temperature region near T_c as shown in Fig. 8. This fact might be an indication that the effect of spin fluctuations on the transport predominates, relative to the lattice vibration effects in $MnGe_4$.

Summary

Two new germanides, $MnGe_4$ and $CoGe_4$, were synthesized under high pressure–temperature conditions. The exact chemical compositions of the prepared specimens were determined to be $Mn_{0.875}Ge_4$ and $Co_{0.975}Ge_4$, respectively. The crystal structures of both compounds were superstructures of the β-$NiHg_4$-type structure. The unit cell of $MnGe_4$ is composed of four β-$NiHg_4$-type cells, and that of $CoGe_4$ is composed of eight β-$NiHg_4$-type cells. The formation of the superstructure might originate from the defect formation at the transition metal sites and from the slight positional changes of the transition metal atoms.
tron ferromagnet with a Curie temperature of 340 K, and is situated in the intermediate region between weakly ferromagnets and nearly localized ferromagnets on the Rhodes–Wohlfarth curve. $CoGe_4$ is a Pauli paramagnetic metal.

References

1. B. ARONSSON, T. LUNDSTRÖM, AND S. RUNDQVIST, "Borides, Silicides and Phosphides," Methuen, London (1965).
2. I. ENGSTRÖM AND B. LÖNNBERG, *J. Appl. Phys.* **63,** 4476 (1988).
3. P. K. PANDY AND K. SCHUBERT, *J. Less-Common Met.* **18,** 175 (1969).
4. V. I. LARCHEV AND S. V. POPOVA, *J. Less-Common Met.* **98,** L1 (1984).
5. H. TAKIZAWA, T. SATO, T. ENDO, AND M. SHIMADA, *J. Solid State Chem.* **68,** 234 (1987).
6. H. TAKIZAWA, T. SATO, T. ENDO, AND M. SHIMADA, *J. Solid State Chem.* **73,** 40 (1988).
7. H. TAKIZAWA, T. SATO, T. ENDO, AND M. SHIMADA, *J. Solid State Chem.* **73,** 427 (1988).
8. R. KUBIAK AND M. WOŁCYRZ, *J. Less-Common Met.* **97,** 265 (1984).
9. R. KUBIAK AND M. WOŁCYRZ, *J. Less-Common Met.* **109,** 339 (1985).
10. J. K. BURDETT, *J. Solid State Chem.* **45,** 399 (1982).
11. T. MATKOVIĆ AND K. SCHUBERT, *J. Less-Common Met.* **59,** P35 (1978).
12. P. ECKERLIN AND H. KANDLER, *in* "Landolt-Börnstein, Numerical Data and Functional Relationships in Science and Technology, New Series" (K. H. Hellwage and A. M. Hellwage, Eds.), Vol. 6, Springer-Verlag, Berlin/Heidelberg/New York (1971).
13. S. OGAWA AND N. SAKAMOTO, *J. Phys. Soc. Japan* **22,** 1214 (1967).
14. D. M. EDWARDS AND E. P. WOHLFARTH, *Proc. R. Soc., Ser. A* **303,** 127 (1968).
15. P. RHODES AND E. P. WOHLFARTH, *Proc. R. Soc., Ser. A* **273,** 247 (1963).
16. E. P. WOHLFARTH, *J. Magn. Magn. Mater.* **7,** 113 (1978).
17. T. MORIYA, *J. Magn. Magn. Mater.* **14,** 1 (1979).
18. K. UEDA AND T. MORIYA, *J. Phys. Soc. Japan* **39,** 605 (1975).
19. K. UEDA, *J. Phys. Soc. Japan* **43,** 1497 (1977).